Biochimica et Biophysica Acta, 448 (1976) 15–33

BBA 77439

LIPID BILAYER ULTRASTRUCTURE

ELECTRON DENSITY PROFILES AND CHAIN TILT ANGLES AS DETERMINED BY X-RAY DIFFRACTION

T. J. McINTOSH, R. C. WALDBILLIG and J. D. ROBERTSON

Department of Anatomy, Duke University School of Medicine, Durham, N.C. 27710 (U.S.A.)

(Received February 25th, 1976)

SUMMARY

High resolution (6 Å) electron density profiles have been computed on an absolute electron density scale for bilayers composed of both saturated fatty acids and fatty acids associated with the alkaline earth series of divalent cations. Low-angle X-ray diffraction data have been interpreted by an isomorphous replacement technique. The position on the X-ray film of discrete wide-angle reflections has provided direct information on the hydrocarbon chain packing and chain tilt in these bilayers. These results have been correlated to an electron microscopy study of the same bilayers (Waldbilling, R. C., Robertson, J. D. and McIntosh, T. J. (1976) Biochim. Biophys. Acta 448, 1–14) and also to X-ray diffraction studies of fatty acid crystals. A method for forming and structurally analyzing bilayers of well defined chemical asymmetry is also described.

INTRODUCTION

Biological membranes are composed primarily of lipids and proteins, with the lipid component thought to exist in a bilayer configuration. Model membrane systems have been extensively analyzed in order to obtain information on the molecular organization of lipid bilayers. In particular, fatty acid bilayers [1–3], phospholipid bilayers [4–6], and protein-lipid complexes [7] have been studied by low-angle X-ray diffraction techniques. Electron microscopy has also been used to a limited extent to study lipid bilayers [8], but interpretation of electron micrographs has in the past been complicated by the unknown effect on bilayer ultrastructure of preparative procedures such as staining, fixing, and embedding. Recently, however, Robertson and Costello [9] and Waldbillig et al. [10] have been able to obtain high resolution micrographs of untreated fatty acid bilayers prepared by the dipping method of Langmuir [11] and Blodgett [12]. Their micrographs indicate that the bilayers are extremely well oriented and that differences in the chemical composition of the lipid head group can be detected by electron microscopy. These recent studies have extended the technique employed earlier by Shidlovsky [13].

Langmuir-Blodgett type bilayers are ideally suited for the X-ray diffraction studies described in this paper. Due to the precise orientation of the bilayers, low-angle diffraction data are recorded at high resolution and wide-angle diffraction spots give direct information on hydrocarbon chain packing and chain tilt. The fact that the chemical composition of the headgroup can be varied allows the X-ray diffraction phase problem to be solved by an isomorphous replacement technique. In addition, absolute electron density scales are calculated from the X-ray diffraction data and are used to interpret the electron density profiles on a molecular level and to correlate them to the electron microscope images of the same bilayers. A further advantage of the Langmuir-Blodgett deposition procedure is that asymmetric bilayers of well defined chemical composition can be built and analyzed by the diffraction techniques.

METHODS

Multilayers with precisely known physical and chemical properties were prepared as described in ref. 10. Usually 50 bilayers were deposited on thin epoxy wafers [10] or thin glass plates. The specimen on the supporting plate was oriented in an oscillation camera (Unicam Instruments, Cambridge, U.K.) so that the planes of the bilayers were approximately parallel to a pinhole collimated X-ray beam. The sample was oscillated through an appropriate angle so that at least the first ten orders of diffraction could be recorded. The specimen was narrow enough that the width of the sample was bathed by the incident beam at all angles of rotation. A rotating anode X-ray generator designed by Dr. William Longley of this laboratory [14] was used to produce copper Kα X-radiation. A pinhole collimator and a nickel filter were used with a flat plate film cassette loaded with three films of Industrial G X-Ray Film (Ilford Ltd., Ilford, Essex, U.K.). Wide angle patterns were recorded by a similar procedure except that the specimen was oscillated through an angle of only 5°. Specimen-to-film distances were between 4 and 8 cm and exposure times usually did not exceed 3 h. All diffraction patterns were recorded at room temperature ($\approx$ 20 °C) and room relative humidity ($\approx$ 50 %).

The diffraction data was processed by standard methods. The discrete low-angle reflections obeyed Bragg's law: $2d \sin \theta = h\lambda$, where d is the repeat period, θ is the Bragg angle, h is the number of the diffraction order, and λ is the wavelength of the X-ray beam. Densitometer traces were recorded on a Joyce-Loebl microdensitometer model MK IIIC (Joyce-Loebl and Co., Burlington, Mass., U.S.A.), the background curve was subtracted, and integrated intensities $I(h)$ were measured. The standard Lorentz-polarization factor for oscillation photographs [15] is $(\cos^2\theta+1)/\sin 2\theta$ and for small angles θ is proportional to $1/h$. Thus, structure amplitudes $F = c\sqrt{hI(h)}$ were obtained where c is a constant. No additional correction factors were used.

RESULTS

Low-angle X-ray diffraction

Low angle X-ray diffraction patterns were recorded from lamellar bilayer systems composed of either long chain fatty acids or of fatty acids saponified with

alkaline earth cations. In addition, diffraction data were collected from oriented barium behenate bilayers which were formed from monolayers which had been spread on subsolutions of various pH and ionic strengths. In all cases, the low-angle pattern consisted of a number of periodic reflections. The lamellar order of the bilayers was judged to be extremely precise as the reflections were quite sharp and showed no appreciable arcing even out to 1/3 Å in reciprocal space.

Bilayers of barium behenate, strontium behenate, and calcium behenate all gave diffraction patterns with a lamellar repeat period of 58 Å. The intensity distribution of the reflections was slightly different in each of the three patterns. Magnesium

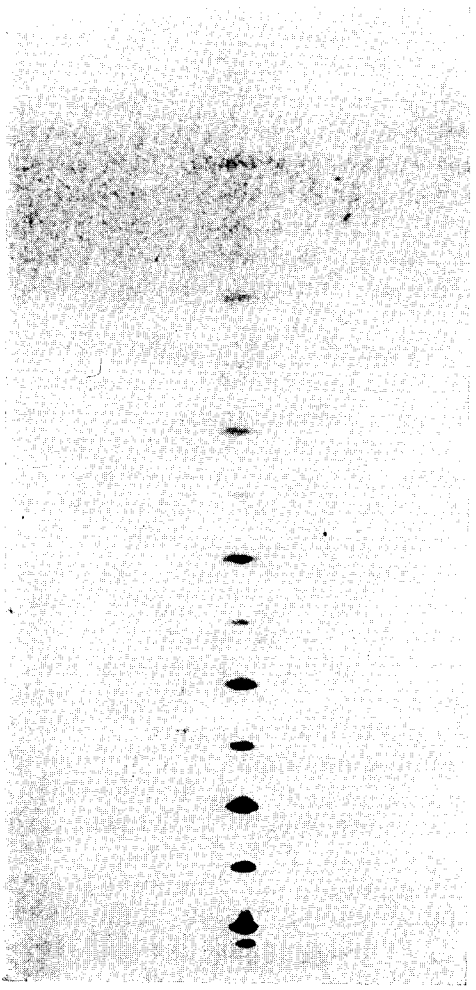

Fig. 1. Low-angle X-ray diffraction pattern from 50 bilayers of barium behenate, $d = 58$ Å. One half of the diffraction pattern is shown and scattering from the beam stop is seen at the bottom of the picture. Extending upward from the beam stop are the first thirteen orders of reflections. The first order, next to the beam stop scatter, is the most intense reflection and, in general, the odd orders are more intense than adjacent even orders. The diffuse scattering around the 13th order comes from the epoxy support.

behenate, on the other hand, had a repeat period of 62 Å while the repeat period from unsaponified behenic acid was 53 Å. For particularly well ordered samples of barium behenate, up to 28 reflections were recorded. Routinely, nine or ten reflections were used in calculations and thus the resolution normally obtained is about 6 Å. A typical diffraction pattern from barium behenate is shown in Fig. 1. Note that the odd orders are, in general, more intense than the even orders.

Wide-angle X-ray diffraction

Two types of wide-angle patterns were recorded depending on the orientation of the specimen relative to the X-ray beam. When the specimen was oriented so that the beam was normal to the plane of the bilayer, several concentric rings were recorded on the X-ray film, with the most intense having spacings of 4.1 and 3.7 Å. When the sample was oriented so that the incident beam was approximately parallel to the planes of the bilayer, the wide-angle diffraction patterns consisted of several sharp, discrete reflections in the case of barium behenate and behenic acid, and two to four diffuse spots for strontium, calcium, and magnesium behenate. In the cases of barium behenate and behenic acid the sharpness and orientation of the discrete reflections makes it possible to infer the type of hydrocarbon chain packing present in the specimen as well as the tilt of the chains relative to the interface. In the following analysis, we will be referring to the wide-angle pattern recorded when the incident beam is parallel to the plane of the bilayers.

The wide angle pattern from barium behenate (Fig. 2A) contains two rows of discrete reflections. The first row corresponds to a spacing of 4.1 Å (as measured from the origin of the film to the center of the row of reflections) and contains three discrete reflections, while the second row is at a spacing of 3.7 Å and also contains three sharp reflections with the middle reflection extremely weak in intensity. The periodicity of the wide-angle reflections within each row is the same as the periodicity of the low-angle reflections (58 Å). These rows of reflections are therefore row lines of a polycrystalline pattern. Since there are discrete, relatively sharp reflections in each row line, there must be a three dimensional order in the multilayer specimen. The sample is undoubtedly polycrystalline, instead of a single crystal, as the wide-angle pattern recorded when the X-ray beam is oriented perpendicular to the planes of the bilayer contains two rings instead of discrete spots. Note that the reflections in both the 4.1 and 3.7 Å row lines are at small angles relative to the equatorial axis of the X-ray film. The angles between the equator and lines drawn from the origin of the film to the center of each row line are approximately 10° and 18°, respectively. There is an additional weak reflection at 2.5 Å which is directly on the equator and is not shown in Fig. 2A.

The reflections in the wide-angle pattern of behenic acid correspond to these same spacings, but have quite a different position (see Fig. 2B). For behenic acid, the 4.1 Å reflection is at an angle of about 22° off the equator while the 3.7 Å reflection is precisely on the equator and is partially obscured by the shadow of the glass support. There is also a weak reflection at a spacing of 2.5 Å which is off the equator by 27° and is not shown in Fig. 2B. Another interesting feature of this pattern is that the 4.1 Å row line on the right of the film contains two discrete reflections, while the row line on the left of the film contains three or four slightly more diffuse reflections which overlap each other. This is a constant feature of wide angle patterns

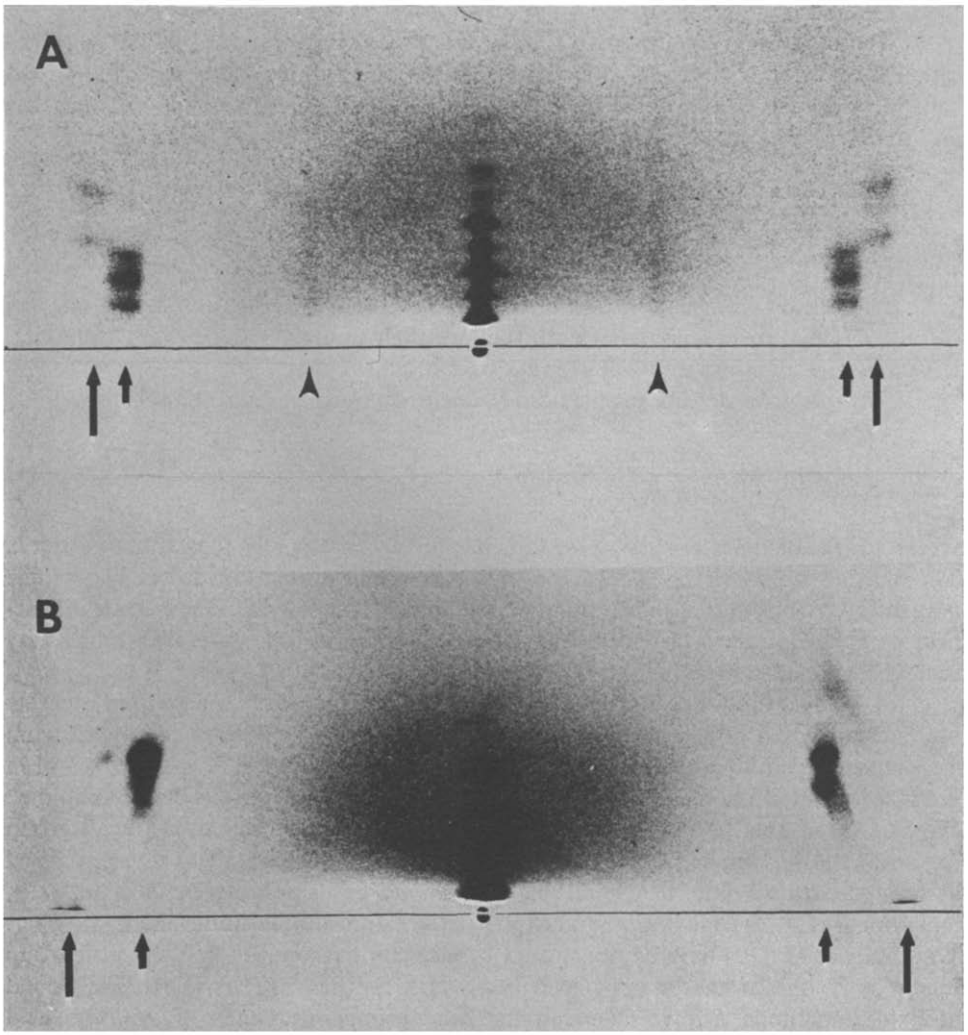

Fig. 2. Wide-angle X-ray diffraction pattern from 50 bilayers of (A) barium behenate and (B) behenic acid. One half of the diffraction pattern is shown and a narrow horizontal black line has been drawn in on the equator at the bottom of each pattern. Before the exposure was taken, the beam stop was removed for a few seconds so that the direct beam is seen in the middle of the equator as a black circle. The light line through the circle is due to absorption by the specimen and glass support. In each pattern the first few low-angle meridional reflections are seen above the main beam and beam stop. The arrows point to the wide-angle reflections. In (A) there are two sets of discrete wide angle-reflections. The inner line of reflections (short arrows) is at a spacing of 4.1 Å, while the outer line of reflections is at a spacing of 3.7 Å (long arrows). Lines drawn from the center of these rows of reflections to the origin (the image of the direct beam) make angles of about 10 and 18°, respectively, with the equator. There is also a diffuse row of reflections at a spacing of 8.2 Å (arrow heads). This 8.2 Å line begins at the equator and extends to the opposite edge of the film. In film (B), the short arrows point to a 4.1 Å reflection which is at an angle of about 27 ° with respect to the equator. The long arrow points to a 3.7 Å reflection which is directly on the equator and is partially obscured by the shadow of the glass support.

from behenic acid and the cause is unknown.

The wide angle patterns show that strontium, calcium, and magnesium behenate bilayers have significantly less long range order. The patterns from these fatty acid salts have diffuse reflections at 4.1 and 3.7 Å and the calcium behenate pattern has additional reflections corresponding to spacings of 4.5 Å and 3.2 Å.

STRUCTURAL ANALYSIS

Electron density profiles

Significant information on the three dimensional organization of the bilayers can be obtained from analysis of both the low-angle and wide-angle diffraction data. Let us first of all consider the low-angle (meridional) pattern.

The electron density profile across a centrosymmetric bilayer is given by

$$\rho(x) \propto \sum_h \phi(h)|F(h)| \cos \frac{2\pi h x}{d} \tag{1}$$

where x is the distance normal to the lamellar surface and $\phi(h)$ is the phase of order h. The phase factors $\phi(h)$ are either $+1$ or -1 for each diffraction order. The profile $\rho(x)$ as given above is on an arbitrary scale. To make full use of the low-angle diffraction data, the phase information must be found and an absolute electron density scale determined.

Lesslauer and Blasie [1] determined the phase factors for barium stearate multilayers by using deconvolution methods on diffraction patterns recorded from a specimen containing a small number of unit cells. In the present study it has been possible to determine the phase angles by an isomorphous replacement technique. We have been able to change systematically the electron density of the head group region of the bilayer in three separate ways. First of all, the kind of divalent metal associated with the fatty acid molecule was altered by using different divalent salts, including $BaCl_2$, $SrCl_2$, $CaCl_2$, and $MgCl_2$, in the subsolution under the monolayer. Waldbillig et al. [10] have demonstrated by electron microscopy that the head group region of the bilayer has different electron densities for these different salts. The second and third methods involve changing the head group occupancy of the fatty acid (that is, the ratio of saponified to unsaponified fatty acids in the bilayer) for one particular divalent salt, such as barium, by changing the pH of the subsolution or by changing the concentration of $BaCl_2$ in the subsolution.

The technique of changing the head group electron density by changing the bulk pH of the subsolution is particularly straightforward in terms of the diffraction analysis. In several previous monolayer studies [16–20], it has been shown that the occupancy of the head group of stearic acid is dependent on the pH of the monolayer subsolution. In the accompanying electron microscope study of oriented bilayers [10] it has been demonstrated that the electron density of the head group region of barium behenate multilayers decreased as the pH of the monolayer subsolution was decreased from pH 9 to pH 4. For determining the phases of the X-ray diffraction reflections, let us consider two particular sets of data, the diffraction patterns recorded from barium behenate bilayers using pH 9 and pH 6. These two particular patterns are ideal to use, as both low-angle patterns consist of sharp

reflections of the same repeat period, but with small differences in intensity distribution. Moreover, the wide-angle patterns of the two specimens are identical, indicating that the chain packing of the fatty acid chains is the same in the two specimens. (The diffraction patterns of specimens formed at pH 4 and pH 5 are not as suitable as they showed considerably more disorder. Multilayers could not be formed at pH values higher than pH 9 as the monolayer film is unstable at these higher pH values.) A method similar to that of Hargreaves [21] was used to determine the phase information for these data sets. Zaccai et al. [22] have used a similar type of analysis to determine the phase information for neutron diffraction studies of lipid bilayers.

Consider two model bilayer systems, A and B, both of repeat period d, which are identical except for the head group region. Assume each head group region to be of uniform electron density, to be of width w, and to be centered at $x = 0$. Let the uniform electron densities of the head group region be labeled ρ_A and ρ_B. The difference in electron density distributions for the two systems is

$$\Delta\rho(x) = \begin{cases} \rho_A - \rho_B & \text{for } -w/2 \leqq x \leqq w/2 \\ 0 & \text{for } -d/2 \leqq x \leqq -w/2 \text{ and } w/2 < x \leqq d/2 \end{cases} \tag{2}$$

The difference in Fourier transforms between these two models is

$$F_A(X) - F_B(X) = \frac{\rho_A - \rho_B}{\pi X} \sin \pi X w \tag{3}$$

where X is the reciprocal space coordinate. Therefore,

$$\frac{\phi_A(h)|F_A(h)|}{\frac{1}{h}\sin\frac{\pi h w}{d}} - \frac{\phi_B(h)|F_B(h)|}{\frac{1}{h}\sin\frac{\pi h w}{d}} = \frac{d}{\pi}(\rho_A - \rho_B) \tag{4}$$

Letting c_A and c_B be scale factors chosen so that the two sets of experimental data $\sqrt{hI_A(h)}$ and $\sqrt{hI_B(h)}$ are normalized to the same scale, then

$$\frac{c_A\phi_A(h)\sqrt{hI_A(h)}}{\frac{1}{h}\sin\frac{\pi h w}{d}} - \frac{c_B\phi_B(h)\sqrt{hI_B(h)}}{\frac{1}{h}\sin\frac{\pi h w}{d}} = \frac{d}{\pi}(\rho_A - \rho_B) \tag{5}$$

Setting

$$A(h) = \frac{\phi_A(h)\sqrt{hI_A(h)}}{\frac{1}{h}\sin\frac{\pi h w}{d}} \tag{6}$$

and

$$B(h) = \frac{\phi_B(h)\sqrt{hI_B(h)}}{\frac{1}{h}\sin\frac{\pi h w}{d}} \tag{7}$$

then

$$c_A A(h) - c_B B(h) = \frac{d}{\pi}(\rho_A - \rho_B) \tag{8}$$

Thus, a plot of $A(h)$ versus $B(h)$ will produce a straight line with slope equal to $(-c_A/c_B)$ if the phase factors $\phi_A(h)$ and $\phi_B(h)$ are chosen correctly for each order and the parameter w can be determined.

The parameter w can be determined from the difference Patterson function, $\Delta P(x)$, where

$$\Delta P(x) = \Delta\rho(x)^* \Delta\rho(x) \propto \sum_h [F_A(h) - F_B(h)]^2 \cos \frac{2\pi h x}{d} \tag{9}$$

and the * symbol stands for the convolution operation. Note that since $\Delta\rho(x)$ is zero for $x \geq w/2$, $\Delta P(x)$ must be zero for $x \geq w$. Thus, w can be determined by examination of the difference Patterson function. In the case of barium behenate for pH 9 and pH 6, and first nine reflections are all quite intense. Since the change in intensity $[I_B(h) - I_A(h)]$ of each reflection is small relative to each reflection intensity $[I_B(h)]$, a change of sign for any reflection is very unlikely. Thus, for this particular case, $\Delta P(x)$ can be written

$$\Delta P(x) \propto \sum_h [|F_A(h)| - |F_B(h)|]^2 \cos \frac{2\pi h x}{d} \tag{10}$$

The difference Patterson function for barium behenate, pH 9 and pH 6, was calculated from Eqn. 10 and is shown in Fig. 3. Note that the $|F_A(h = 0)|$ and $|F_B(h = 0)|$ terms are not experimentally observable so that the curve of Fig. 3 is on an abitrary

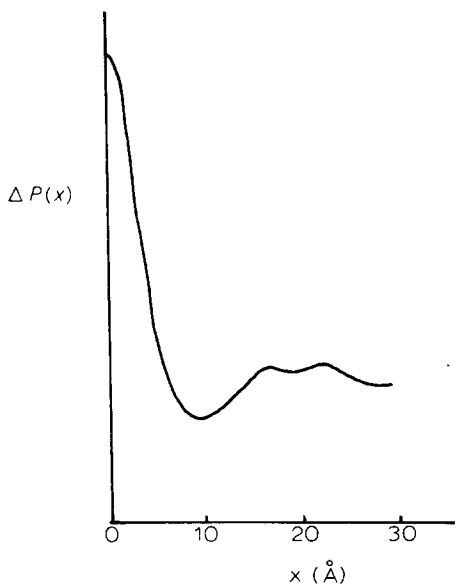

Fig. 3. Difference Patterson function computed using the first nine orders of diffraction from barium behenate bilayers formed using 10 mM $BaCl_2$ subsolutions at pH 9 and pH 6.

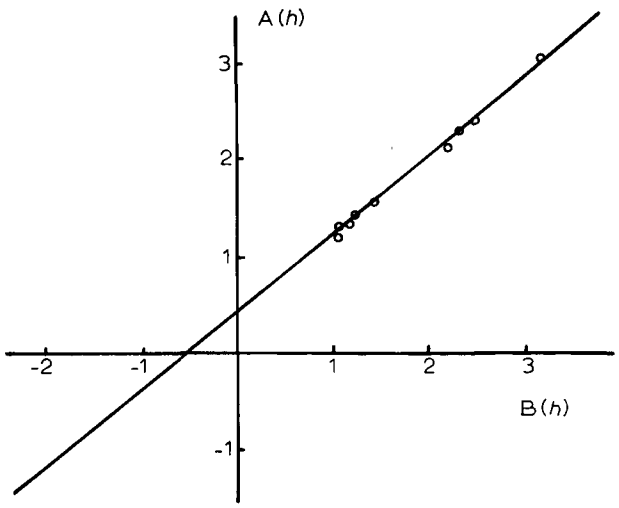

Fig. 4. Hargreaves' plot for the first nine orders of diffraction from barium behenate bilayers formed using 10 mM $BaCl_2$ subsolutions at pH 9 and pH 6. All positive phase factors were used. From left to right, the open circles represent the following diffraction orders, $h = 6, 8, 2, 4, 1, 3, 5, 7$, and 9.

ordinate scale. There is one major peak in this curve, centered at $x = 0$. This means that at this resolution the head group density is centered at the origin. The curve abruptly drops to a constant value when $x \geqslant 5$ Å, and then levels off. Since the $h = 0$ terms are not included in the calculation of $\Delta P(x)$ by Eqn. 10, this constant value is equal to $-[|F_A(0)|-|F_B(0)|]^2$. The fact that the curve abruptly drops to this constant value at $x \geqslant 5$ Å means that $w \leqslant 5$ Å.

In Fig. 4, $A(h)$ and $B(h)$ have been plotted using intensities from barium behenate bilayers deposited at pH 9 and pH 6, respectively, with all positive phase factors $\phi_A(h)$ and $\phi_B(h)$ in Eqns. 6 and 7. Clearly $A(h)$ and $B(h)$ fall on a straight line, implying that this is the correct phase combination for all diffraction orders. There exists one possible ambiguity in that a phase combination of all negative phase factors would also produce a straight line. However, this ambiguity can be removed by examination of the coordinate intercepts of the straight line. Note from Eqn. 8 that when $B(h) = 0$, $A(h) = d(\rho_A-\rho_B)/\pi c_B$ and that when $A(h) = 0$, $B(h) = -d(\rho_A-\rho_B)/\pi c_A$. From surface chemistry [16] and electron microscopy studies [10] it is known that the head group electron density of barium behenate deposited at pH 9 (ρ_A) is greater than that at pH 6 (ρ_B). Thus, $\rho_A-\rho_B$ is positive. Since c_A and c_B are also positive, this means that for the correct phase combination $A(h)$ is positive when $B(h) = 0$ and $B(h)$ is negative when $A(h) = 0$. Clearly from Fig. 4, this is the case for the all positive phase combination. Thus, the first nine orders of diffraction from barium behenate, at either pH 9 or pH 6, all have positive phase factors. Note that this is the equivalent phase combination determined by Lesslauer and Blasie [1] for barium stearate bilayers.

Electron density plots for barium behenate bilayers at pH 9 and pH 6 are shown in Fig. 5. These curves are on the same relative scale as the ratio of scale factors c_A/c_B which was obtained from the slope of the straight line of Fig. 4. The

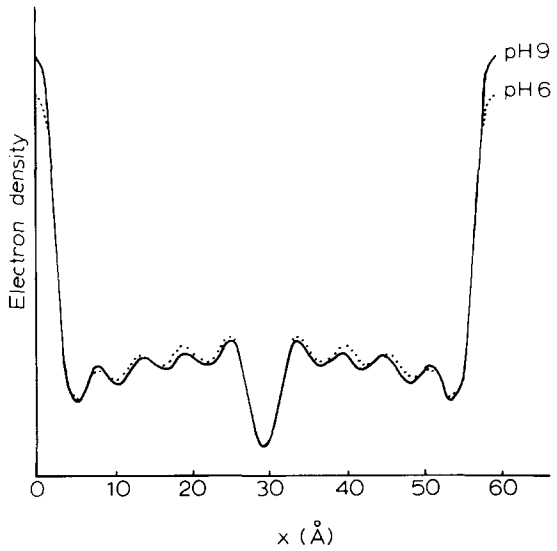

Fig. 5. Electron density profiles for barium behenate bilayers formed using 10 mM $BaCl_2$ subsolutions at pH 9 (solid curve) and pH 6 (dotted curve). Nine orders of diffraction were used in these Fourier synthesis and the resolution is 6.5 Å. The hydrocarbon regions of the bilayer, from $x \simeq 5$ Å to $x = 53$ Å, superimpose closely, while the head group regions, centered at $x = 0$ Å and $x = 58$ Å, have different electron densities due to different barium occupancies of the head groups.

profiles show the high electron density head group regions centered at $x = 0$ and at $x = d$. The regions of relatively uniform electron density between the head group peaks correspond to the hydrocarbon chain region of the bilayer. The sharp dip in electron density in the center of the bilayer has been attributed to the registration of the terminal methyl groups of the hydrocarbon chains [1]. Note that in Fig. 5 the hydrocarbon regions of the two bilayers superimpose almost exactly. However, the head group region of barium behenate formed at the higher pH is slightly more electron dense.

The phase problem for the diffraction data from the other specimens is now quite straightforward to solve, either by a rigorous isomorphous replacement analysis as above, or by the trial and error method of choosing the phase combination which gives the most similar hydrocarbon chain region as the curves of Fig. 5. The isomorphous replacement analysis has been performed for several data sets, including barium behenate formed over subsolutions of different ionic strengths, as well as for strontium and calcium behenate. The results are always equivalent to those described above. A plot of electron density profiles of barium behenate bilayers which were deposited from monolayers formed over subsolutions containing various concentrations of $BaCl_2$ at pH 9 is shown in Fig. 6. Again the hydrocarbon chain regions for the different profiles superimpose quite closely. The head groups of the profiles of bilayers formed over 100 mM and 10 mM $BaCl_2$ subsolutions are very close in electron density, while the head groups of the bilayers formed over 1 mM and 0.1 mM are considerably lower. It has been shown in previous studies [16, 20] that in the case of stearic acid there is nearly full conversion of fatty acid carboxyl to saponified

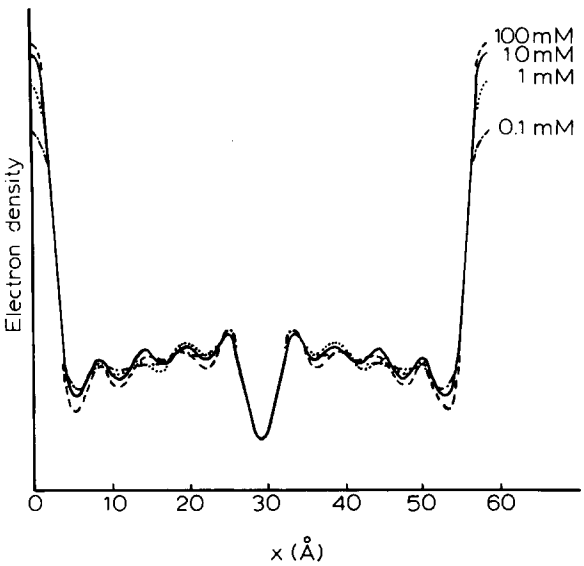

Fig. 6. Electron density profiles for barium behenate bilayers formed using $BaCl_2$ (pH 9) subsolutions at the following concentrations: 100 mM (dashed curve), 10 mM (solid curve), 1 mM (dotted curve), and 0.1 mM (dash-dot curve). The hydrocarbon regions of the bilayers superimpose closely, but the head group regions have different electron densities due to different barium occupancies of the carboxyl group.

fatty acid carboxylate at $BaCl_2$ concentrations of $\leqslant$ 10 mM at pH 9. By assuming full occupancy for the 100 mM $BaCl_2$ headgroup (that is, 0.5 barium ions per lipid molecule) and zero barium occupancy for the behenic acid head group, it can be estimated that the number of barium ions per lipid molecule is 0.49, 0.44, and 0.39 for bilayers formed over 10 mM, 1 mM, and 0.1 mM concentrations. Note that Fig. 6 is the X-ray diffraction analog to the electron micrograph which Waldbillig et al. [10] show in their Fig. 5.

An absolute electron density scale can be determined by comparison of data from barium behenate and unsaponified behenic acid bilayers (Fig. 9). Profiles of barium behenate (10 mM, pH 9) and behenic acid bilayers were put on the same relative scale by superimposing their hydrocarbon chain regions. An absolute electron density scale was then determined from theoretical calculations of the head group electron densities of the two profiles. Since the area per molecule is known from monolayer data [16, 20] and from the wide angle diffraction results (see next section), and the width of the head group can be estimated from the profiles of Fig. 9, it follows that the volume of the head group region can be calculated. Assuming that the entire carboxyl moiety is in the head group region, the number of electrons localized in head group regions of the bilayer is known for both barium behenate and behenic acid and their theoretical electron densities can be calculated. These head group electron densities are 1.02 e/Å^3 for barium behenate (assuming 0.49 barium ions per lipid at 10 mM, pH 9) and 0.49 e/Å^3 for behenic acid. From these two values, an absolute electron density scale has been computed for the barium behenate bilayer and is shown in Fig. 9. This scale is similar to one obtained for

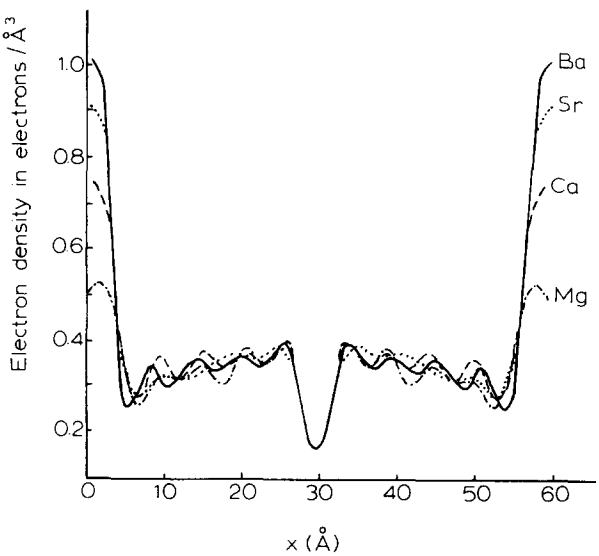

Fig. 7. Electron density profiles for barium behenate (solid curve), strontium behenate (dotted curve), calcium behenate (dashed curve), and magnesium behenate (dash-dot curve). The profiles have been put on an absolute electron density scale as described in the text.

barium stearate bilayers by Lesslauer [2].

In Fig. 7, Fourier syntheses of strontium behenate, calcium behenate, and magnesium behenate were put on the same absolute scale as barium behenate by superimposing their hydrocarbon chain regions. The head group regions vary in electron density in agreement with the electron microscopic studies [10]. For a consistency check, theoretical absolute electron densities for the strontium, calcium, and magnesium head groups can be calculated and compared to the scale determined for barium behenate. Assuming 0.5 divalent cations per lipid molecule and placing the carbon and two oxygen atoms from the carboxyl group in the head group volume, the following head group electron densities are calculated: Sr 0.88 e/Å^3, Ca 0.69 e/Å^3, and Mg 0.60 e/Å^3. These calculated values of head group electron densities are in quite good agreement with the heights of the head group profiles on the absolute scale of Fig. 7. The height of the head group profile for strontium behenate matches the calculated value quite closely, while the profile for calcium is slightly higher than the calculated value and the magnesium profile is slightly lower. These small differences could be caused by several factors. First of all, the number of divalent cations per lipid molecule might be slightly different than 0.5 for each particular cation. There also might be some bound water molecules in the head group regions, particularly in the cases of calcium and magnesium behenate. The magnesium behenate bilayer has a larger repeat period than the other saponified fatty acids. As can be seen from the electron density plots of Fig. 7, this is because there is an extra layer of relatively low electron density at the outer edges of the bilayer. This has been attributed to a layer of water attached to the magnesium head group [2]. This extra hydration layer complicates the analysis as the height of the head group region in a limited resolution Fourier synthesis might be altered by an extra layer between the

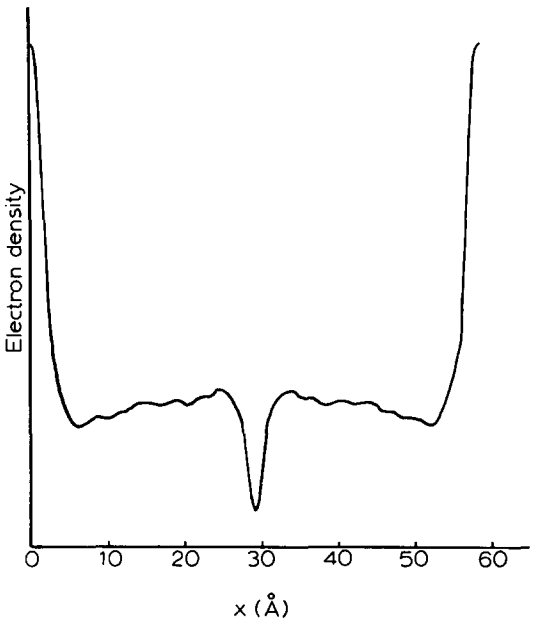

Fig. 8. Electron density profile for barium behenate formed at 10 mM $BaCl_2$ concentrations (pH 9) using the first 21 diffraction orders. The resolution of the profile is 2.8 Å.

bilayers. In addition, there are small experimental uncertainties in measuring integrated intensities and in the procedure of superimposing hydrocarbon chain regions to put different profiles on the same graph.

A rigorous structural analysis has only been performed for the first nine orders of barium behenate. However, the intensities for orders 10–21 have the same sort of intensity distribution as the lower orders, that is, the even numbered reflections are much less intense than the odd orders. According to the arguments of Lesslauer and Blasie [1] this indicates that orders 10–21 have the same phase (positive) as orders 1–9. All positive phase factors were used to compute the electron density plot for barium behenate at 3 Å resolution that is shown in Fig. 8. Note that this plot looks very similar to the previous plots at 6 Å resolution (Fig. 5), but the Fourier ripple has smoothed out considerably. The prominent features are the same, except that the terminal methyl trough and the head group peak have become slightly narrower and a small shoulder has appeared at the base of the head group peak. This shoulder might be a Fourier ripple artifact, or it may represent a portion of the carboxyl moiety of the head group.

Chain packing and chain tilt

The position on the film of the wide-angle reflections gives direct information on chain tilt as the strongest reflections will be perpendicular to the reflecting planes which contain the lipid molecules. Quantitatively, analysis of the wide-angle data is considerably simplified as it can be directly correlated with crystallographic results. Crystals of n-fatty acids with even numbers of carbons atoms in their chains have three polymorphic forms, commonly labelled A, B, and C [23]. Saturated fatty acids

containing more than 16 carbons usually form crystals of the B or C type. The first single crystal studies were of the B form of stearic acid [24, 25] and for the C form of lauric acid [26]. There have been several subsequent studies, and the cell dimensions of both polymorphs of stearic acid have been obtained. In the B form at 20 °C, the unit cell is monoclinic with $a = 5.59$ Å, $b = 7.40$ Å, $c = 49.38$ Å, and $\beta = 117°22'$. The subcell, which is used to describe the hydrocarbon chain packing in the crystal [23], is orthorhombic with $a_s = 4.96$ Å and $b_s = 7.40$ Å. The subcell dimensions are consistent with those obtained from lead stearate multilayers by electron diffraction [27]. In the C form, the unit cell is monoclinic with $a = 9.36$ Å, $b = 4.96$ Å, $c = 50.75$ Å, and $\beta = 128°16'$ and the subcell is orthorhombic with $a_s = 7.40$ Å and $b_s = 4.96$ Å [23]. In other words, in both the B and C forms of stearic acid crystals, the chains are packed in an orthorhombic subcell. However, in the B form the structure is tilted over the long subcell axis (7.40 Å) giving an increase in the length of the short axis of the unit cell from 4.96 to 5.59 Å, while in the C form the structure is tilted over the short subcell axis (4.96 Å) giving an increase in the length of the long axis from 7.40 to 9.36 Å [28]. It has been noted that the B form can be converted irreversibly to the C form by heating the crystal to within 5 °C of its melting point [23].

The wide-angle pattern from behenic acid bilayers (Fig. 2B) is completely consistent with the crystallographic data of the B form of stearic acid. The 4.1, 3.7, and 2.5 Å row line reflections from the oriented behenic acid bilayers correspond to the (11*l*), (02*l*), and (20*l*) row lines from the stearic acid crystal. The location of the 3.7 Å bilayer reflection on the equator and the 4.1 and 2.5 Å reflections off the equator by 22 and 27°, respectively, is consistent with a model in which the hydrocarbon chains of the bilayer are tilted 117° relative to the short axis ($a = 5.59$ Å)of the unit cell and are at right angles to the $b = 7.40$ Å axis of the unit cell. That is, the chains are tilted 27° relative to the normal to the plane of the bilayer. (Note that the crystallographic parameter β gives the angle between sides a and c of the unit cell. However, in the case of lipid bilayers it is customary to consider chain tilt relative to the normal to the plane of the bilayer.) The positions of the (11*l*), (20*l*), and (02*l*) layer lines on the X-ray film (Fig. 2B) can be explained by calculation of the angles between reflecting planes. From the formula given in ref. 29, it is found that for this monoclinic unit cell the (001) reflecting planes make angles of 68, 63, and 90° with respect to the (110), (200), and (020) reflecting planes respectively. For the Langmuir-Blodgett type multilayers, the planes of the bilayer are equivalent to the (001) reflecting planes. In this polycrystalline specimen the bilayers are oriented so that the planes of the bilayer are all very nearly parallel, but there is no preferred angular orientation of the crystallites about an axis perpendicular to these planes. Thus, when the planes of the bilayer are oriented parallel to the X-ray beam and parallel to the equator of the X-ray film, the (110), (200), and (020) reflections should be observed at angles of 22, 27, and 0° relative to the equator of the X-ray film. The X-ray pattern (Fig. 2B) does contain strong reflections at these angles. There are other reflections on the film, particularly in the (11*l*) row line, but from crystallographic data [25] the (110), (200), and (020) reflections are expected to be the strongest.

In order to convert it to the C form, the specimen of behenic acid bilayers was heated to 75 °C, 5 °C below the melting temperature, and then allowed to slowly return to room temperature ($\approx$ 20 °C). After this procedure, the low-angle diffraction

pattern contained a series of reflections with a periodicity of 48 Å, which is 5 Å shorter than the repeat period before heating. Although the repeat period changed, the intensity distribution of the low-angle reflection was almost identical before and after heating procedure. However, the wide-angle pattern of the heated specimen did change to consist of two spots, one at a spacing of 4.1 Å located at an angle of about 22° relative to the equator, and the other at 3.7 Å and off the equator by about 38°. These spots correspond to the (110) and (200) reflections from the C form of the fatty acid crystal. Again, the positions of these reflections on the X-ray film can be explained by calculation of the angles between the reflecting planes. The angle between the (001) and (110) reflecting planes is 68° and the angle between the (001) and (200) reflecting planes is 52°. Thus, for the sample geometry used in these experiments, the (110) and (200) reflections should be located off the equator by 22° and 38° respectively, exactly as they are on the X-ray film. Thus, in the bilayer C form, the chains are tilted 128° relative to the $a = 9.36$ Å axis of the unit cell and are perpendicular to the short axis ($b = 4.96$ Å) of the unit cell. In other words, in this case the chains are tilted 38° relative to the normal to the plane of the bilayer.

Electron density profiles for behenic acid bilayers, in both the B and C forms, are given in Fig. 9. Note the profiles are very similar in shape, with the major difference being that the C form is narrower. The difference in repeat period between the B and C forms of behenic acid can be attributed to the differences in hydrocarbon chain tilt. It can be estimated from crystallographic data [30], that if a bilayer were formed from two fully extended behenic acid molecules oriented perpendicular to the plane of the bilayer it would have width of about 61 Å. The B form, which has a measured chain tilt of 27°, should have a width of 54 Å (since 54 Å = 61 Å cos 27°) and the C form, which has a chain tilt of 38°, should have a width of 48 Å (since 48 Å = 61 Å

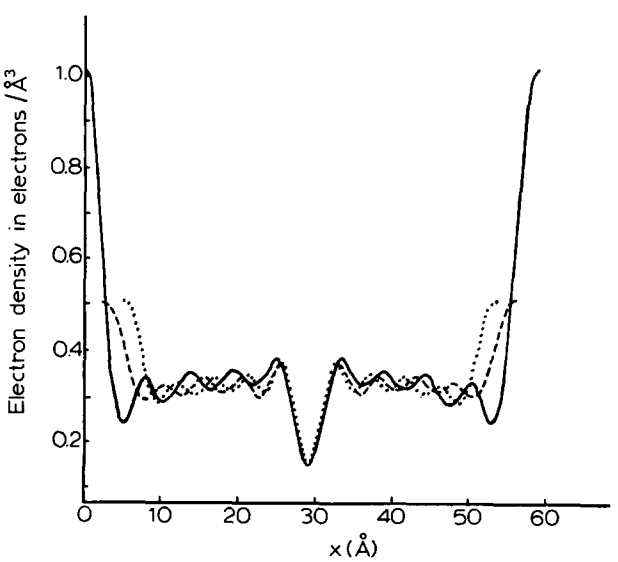

Fig. 9. Electron density profile for barium behenate (solid curve), the B form of behenic acid (dashed curve), and the C form of behenic acid (dotted curve). The profiles have been put on an absolute electron density scale.

cos 38°). These widths are quite close to the experimentally measured repeat periods of 53 and 48 Å. Note also that the repeat period for barium behenate of 58 Å corresponds to a bilayer with a much smaller chain tilt (about 18°),which is consistent with the wide-angle pattern for barium behenate bilayers (Fig. 2A). In the case of barium behenate bilayers, the chains are tilted over the short subcell axis (4.96 Å) giving an increase in the length of the long axis from 7.40 Å to about 7.8 Å.

The orthorhombic subcell for both the B and C forms of behenic acid has dimensions of 4.96 Å and 7.40 Å. The wide-angle reflections from barium behenate bilayers are also consistent with this subcell. Since there are two molecules per subcell [23], the area per molecule in the subcell is 18.35 $Å^2$. The area per molecule in the plane of the bilayer is therefore 18.35 $Å^2/\sin \beta$ and is equal to 19.3 $Å^2$ for barium behenate and 20.7 $Å^2$ and 23.2 $Å^2$ for the B and C forms of behenic acid. These results are consistent with previous monolayer surface chemistry studies [16, 20].

The two extra reflections recorded from calcium behenate bilayers at 4.5 and 3.2 Å have spacings in the ratio of $\sqrt{2}$. This implies that some of the calcium behenate molecules might be oriented in a square array, much like that proposed by Deamer and Cornwell [31].

In Fig. 2A, there is an extra row line at a spacing of 8.2 Å which is similar in shape to a row line on a Bernal chart [32]. The origin of this line is uncertain and it has been only observed in the case of barium behenate specimens. Since there are two lipid molecules for every barium ion [16] and since there is a strong reflection from the lipid chains at 4.1 Å, it seems possible that the 8.2 Å row line might be caused by the barium ions in the specimen.

Asymmetric bilayers

Another interesting study that can be performed with the techniques described in this paper is the analysis of asymmetric bilayers. Asymmetric bilayers can be deposited on supports by the Langmuir-Blodgett technique if monolayer films are alternated on successive dipping cycles [10]. Due to the procedure of deposition, the one dimensional unit cell contains two bilayers with a center of symmetry between adjacent bilayers [10], and therefore, this system can be analyzed by X-ray diffraction methods.

The first asymmetric bilayer studied consisted of apposing monolayers of behenic acid and barium behenate. This is an intriguing case to analyze, as the width of a monolayer of behenic acid is less than a monolayer of barium behenate. Moreover, the chain tilt and the head group electron densities are different in the two cases. The diffraction pattern from a specimen containing 25 oriented asymmetric bilayers consists of 18 sharp diffraction orders of a periodicity of 112 Å. The phase information is easily obtained since the structure of each apposing monolayer is already known (Fig. 9). The electron density profile for this asymmetric bilayer is shown in Fig. 10. Several points should be noted. First of all, the bilayer is indeed asymmetric, as the head group electron density on the barium behenate side is considerably greater than that of the behenic acid side. However, the difference in electron densities between the two sides is not as great as one would expect from apposing monolayers of pure behenic acid and pure barium behenate. A possible explanation of this is a small amount of translational diffusion or "flip-flop" across the bilayer either during

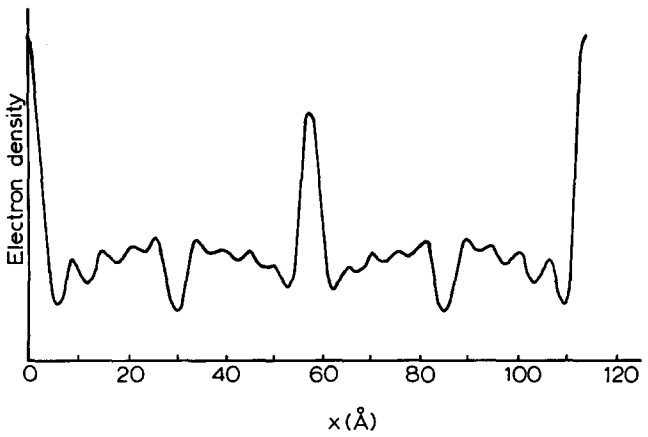

Fig. 10. Electron density profile for asymmetric bilayers containing apposing monolayers of barium behenate and behenic acid computed using the first 18 orders of diffraction. One unit cell, $d = 112$ Å, which contains two asymmetric bilayers is shown.

or after the formation of the bilayers. See Waldbillig et al. [10] for a more complete discussion of this point. Also, note that the width of the barium behenate monolayer is greater than that of the behenic acid monolayer. That is, the terminal methyl dip in each bilayer is asymmetrically situated with respect to the center of the bilayer as it is about 1.5 Å closer to the behenic acid headgroup than to the barium behenate head group. The terminal methyl trough can be located even more asymmetrically with respect to the center of the bilayer by building asymmetric bilayers composed of apposing monolayers of barium behenate and barium palmitate (McIntosh and Waldbillig, unpublished results).

DISCUSSION

The electron density profiles for the fatty acid salts (Fig. 7) are completely consistent with the electron microscope results [10], but at a higher resolution (6 Å). In addition, the electron density distributions have been put on an absolute electron density scale. The narrow high density peaks at both edges of the bilayer represent the carboxylate group of the fatty acid. The absolute electron densities of these peaks are consistent with calculations made assuming that two fatty acid molecules interact with each divalent cation. The electron densities of these head group peaks qualitatively match the relative densities of the electron microscope images of the same divalent salts [10]. The high density head group peak is considerably narrower (approx. 2.5 Å) in the calculated electron density profiles than the high density region in the electron micrographs. This is probably due primarily to the fact that the X-ray diffraction patterns are at a considerably higher resolution than the electron micrographs. The resolution of the electron density profile is 6 Å, while the resolution of the electron micrographs has been estimated to be about 18 Å from optical diffraction analysis [10]. The profiles also contain flat regions at an electron density of about 0.34 e/Å^3 (Fig. 7) which correspond to the hydrocarbon chain region of the lipids. This value is completely consistent with single crystal studies, as the volume

per CH_2 group in crystals of stearic acid is 23.3 $Å^3$ [23], which corresponds to an electron density of 0.343 e/$Å^3$. The deep low-electron density troughs in the middle of the bilayer have been attributed to the alignment of the terminal methyl groups of the hydrocarbon chains. The narrowness and depth (approx. 0.15 e/$Å^3$) of this trough indicate that the methyl ends of the lipids must be quite well oriented. Analysis of asymmetric bilayers shows that this terminal methyl dip is a "real" structure and not a Fourier series artefact, as the dip is asymmetrically placed in bilayers constructed of apposing monolayers of different chain lengths. The average electron density of the behenic acid bilayers (Fig. 9) is about 0.34 e/$Å^3$ which corresponds to a mass density of 1.00 gm/cm^3. For comparison, the calculated mass densities of crystals of the B-form and C-form of stearic acid [25, 27] are 1.04 gm/cm^3 and 1.02 gm/cm^3, respectively.

Both the low-angle and wide-angle diffraction results indicate that the fatty acid molecules are packed in a very similar manner in the bilayer and in the crystal forms. In both cases, the chains are packed in an orthorhombic subcell and are tilted relative to normal by an angle of 27 or 38°, depending on which polymorphic form the fatty acid is in. The difference in repeat period between saponified and unsaponified fatty acid bilayers is due primarily to the larger degree of chain tilt in the case of the acid. The chain tilt in the case of barium behenate bilayers has been measured to be about 18°.

Thus, the combined low-angle and wide-angle diffraction data gives a three-dimensional picture of the organization of the fatty acid bilayers. The hydrocarbon chains are rigid, tightly packed in an orthorhombic subcell, and tilted relative to the normal to the plane of the bilayer. The terminal methyl groups at the end of the fatty acid chains are in alignment in the center of the bilayer. The head group moieties are also well oriented at the outer edge of the bilayer. Although there is a fluid layer of about 4 Å in width between magnesium behenate bilayers, there is no indication of a low density space between barium behenate bilayers, even in profiles at 3 Å resolution.

ACKNOWLEDGEMENTS

We wish to thank Dr. W. Longley and Dr. M. J. Costello for very helpful discussions during the preparation of this manuscript. This work was supported by grants from the National Institutes of Health (Program Project Research Grant 5 PO1 NS 10299 and Institutional Research Fellowship 1 T22 GM00100). R. C. Waldbillig is a Fellow of the National Multiple Sclerosis Society.

REFERENCES

1 Holley, C. (1936) Phys. Rev. 53, 534–537
2 Lesslauer, W. and Blasie, J. K. (1972) Biophys. J. 12, 175–190
3 Lesslauer, W. (1974) Acta Cryst. B30, 1927–1931
4 Tardieu, A., Luzzati, V. and Reman, F. C. (1973) J. Mol. Biol. 75, 711–733
5 Levine, Y. K., Bailey, A. I. and Wilkins, M. H. F. (1968) Nature 220, 577–578
6 Hitchcock, P. B., Mason, R. and Shipley, G. G. (1975) J. Mol. Biol. 94, 297–299
7 Mateu, L., Luzzati, V., London, Y., Gould, R. M., Vosseberg, F. G. A. and Olive, J. (1973) J. Mol. Biol. 75, 697–709

8 Stoeckenius, W. (1962) J. Cell Biol. 12, 221–229
9 Robertson, J. D. and Costello, M. J. (1974) Eighth International Congress on Electron Microscopy, Canberra, Vol. II, 218–219
10 Waldbillig, R. C., Robertson, J. D. and McIntosh, T. J. (1976) Biochim. Biophys. Acta 448, 1–14
11 Langmuir, I. (1920) Trans. Faraday Soc. 15, 62
12 Blodgett, K. B. (1935) J. Am. Chem. Soc. 57, 1007
13 Schidlovsky, G. (1965) Lab. Invest. 14, 475–494
14 Longley, W. and Miller, R. (1975) Rev. Sci. Instrum. 46, 30–32
15 Lipson, H. (1967) in International Tables for X-ray Crystallography (Kasper, J. S. and Lonsdale, K., eds.), Vol. II, pp. 265–270
16 Langmuir, I. and Schaefer, V. J. (1936) J. Am. Chem. Soc. 58, 284–287
17 Sasaki, T. and Muranatsu, M. (1956) Bull. Chem. Soc. Jap. 29, 35–40
18 Bagg, J., Anderson, M. B., Fickman, M., Haber, M. D. and Gregor, H. P. (1964) J. Am. Chem. Soc. 86, 2759–2763
19 Ellis, J. W. and Pauley, J. L. (1964) J. Colloid Sci. 19, 755–764
20 Deamer, D. W., Meek, D. W. and Cornwell, D. G. (1967) J. Lipid Res. 8, 255–263
21 Hargreaves, A. (1946) Nature 158, 620
22 Zaccai, G., Blasie, J. K. and Schoenborn, B. P. (1975) Proc. Nat. Acad. Sci. U.S.A. 72, 376–380
23 Chapman, D. (1965) The Structure of Lipids, pp. 221–256, John Wiley and Sons, Inc., New York
24 Muller, A. (1932) Proc. Roy. Soc. 138A, 514
25 Von Sydow, E. (1955) Acta Cryst. 8, 557–560
26 Vand, V., Morley, W. M. and Lomer, T. R. (1951) Acta Cryst. 4, 324–329
27 Stephens, J. F. and Tuck-Lee, C. (1969) J. Appl. Cryst. 2, 1–10
28 Degerman, G. and Von Sydow, E. (1959) Acta Chem. Scand. 13, 984–988
29 Donnay, J. D. H. and Donnay, G. (1967) in International Tables for X-ray Crystallography (Kasper, J. S. and Lonsdale, K., eds.), Vol. II, p. 107
30 Abrahamsson, S. and Von Sydow, E. (1954) Acta Cryst. 7, 591–592
31 Deamer, D. W. and Cornwell, D. G. (1966) Biochim. Biophys. Acta 116, 555–562
32 Evans, H. T. and Lonsdale, K. (1967) in International Tables for X-ray Crystallography (Kasper, J. S. and Lonsdale, K., eds.), Vol. II, pp. 175–185